



International Conference on Robotics and Smart Manufacturing (RoSMa2018)

A Low Cost Underwater Robot with Grippers for Visual Inspection of External Pipeline Surface

M. Manjunatha^a, A. Arockia Selvakumar^b, Vivek P Godeswar^c, R. Manimaran^{d*}

^{a,b,c,d} School of Mechanical and Building Sciences, Vellore Institute of Technology, Chennai, Tamil Nadu, India 600127

Abstract

Underwater robots are used in surveillance, academic and military applications because of their capability to execute risky tasks underwater without human intervention. In this study, a robot is built at low cost budget to carry out inspection at specified depth in a water body. Preliminary studies are performed to understand the buoyancy and stability of an underwater robot. Different configurations of propeller arrangements are identified and the final prototype is arrived after meeting the specific application requirements. Dual grippers are incorporated with the underwater robot, one for holding the pipe to avoid underwater currents and other for gripping/releasing the pipe. Gyroscope sensor is embodied in the underwater robot to maintain stability from its feedback signals. A high definition camera is mounted in front of the underwater robot for live video and image capturing purposes. Thus the underwater robot is able to meet all its requirements with minimal frontal drag. For validation purpose, computational fluid dynamics (CFD) studies are carried out with dynamic meshes and boundary conditions. The deviation between CFD and experimental results is found to be within the acceptable limits. The detailed cost analysis for the construction and testing of this underwater robot is also briefly tabulated.

© 2018 The Authors. Published by Elsevier Ltd.

This is an open access article under the CC BY-NC-ND license (<https://creativecommons.org/licenses/by-nc-nd/4.0/>)

Peer-review under responsibility of the scientific committee of the International Conference on Robotics and Smart Manufacturing.

Keywords: Underwater robot; propeller requirement; gripper; Computational fluid dynamics; Image capturing.

1. Introduction

Nomenclature

UUV	Unmanned Underwater Vehicle	ROV	Remotely Operated Vehicle
AUV	Autonomous Underwater Vehicle	HROV	Hybrid Remotely Operated Vehicle
CFD	Computational Fluid Dynamics	CT	Computed Tomography
DOF	Degree Of Freedom	UDF	User Defined Function

* Manimaran R.Tel.: +91-44-39931426; fax: +91-44-39931555.

E-mail address : manimaran.nr@gmail.com

The history of underwater vehicles begins with first manned vehicle prototype by Englishman William Bourne in 1978. The underwater vehicles are classified into two categories; manned and unmanned underwater vehicles. The US Navy defined Unmanned Underwater Vehicle (UUV) as “self-propelled submersible whose operation is either fully autonomous or under minimal supervisory control and untethered except, possible for data links such as a fiber-optic cable” [1]. The ROV has four major parts such as control console, monitor, controller and submersible vehicle which are connected through a long cable to control console. The design structure can observe from [2]. Due to recent advancements in the ROV technologies, camera for visual inspection, robotic arm to perform specific task or action [3] and various advanced sensors are implanted into ROV [4] such that it can work under the environmental conditions where human finds it difficult to work. The ROV can be deployed for the applications like subsea pipeline transportation system [5] in two ways. First, sending a robot in pipeline and scanning the walls by using ultrasonic technology, laser technology etc. But the drawback of this method is when the maintenance process is going on the transportation process should be stopped and this creates a huge loss in the economy for an oil company. Secondly, sending the vehicle to scan and repair the subsea pipeline from the outside without removing the protective layer of the pipe [6]. This process is considered by many and Tracerco (shown in Figure 1) inspects the subsea pipeline inspection underwater vehicle by scanning the outer surface. This vehicle is implemented with CT to facilitate the inspection of subsea pipelines [7]. It is also embedded with a high resolution camera for visual confirmation in critical conditions.

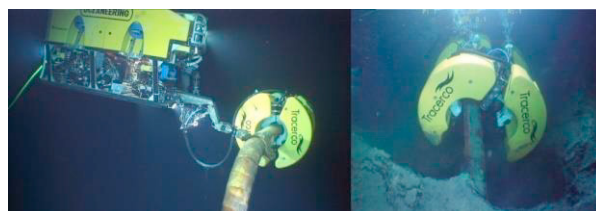


Fig. 1. Courtesy Tracerco for subsea pipeline inspection [7].

The attention on the underwater vehicle structure, control system, visibility in underwater and feasibility in software needs improvement [8, 9]. From the literature, studies are involved with rugged structures operating in a deep environment. These ROV's are very expensive in manufacturing and require significant power during operation. However the present study discusses about the construction of a simplified (lower cost and less operating power) underwater robot that can inspect the external surface of underwater pipeline visually. A pair of grippers are developed to hold/release and to cling along the pipe when the vehicle is moving along the pipe. CFD simulations are also carried out to validate the experimental study.

2. Methodology

2.1. Geometry model and construction

The underwater vehicle consists of a total of five thrusters; two thrusters for surge motion and three thrusters for heave motion and also for sway motion. The geometry of the final prototype is shown in Figure 2 and geometry of the underwater vehicle total length is 0.7 m, height is 0.2 m and width is 0.3 m, the summarized vehicle body parts geometry in Table 1. The underwater robot is divided into body, thruster [5] and gripper [9]. The construction of the underwater robot [10, 11] is started with weight balance of body (stability) using a standard PVC pipe. Additional weight is needed to maintain the body in equilibrium (i.e at a certain depth) in order to overcome buoyancy and self-weight. A single thruster consists of DC motor with four blade propeller. Multiple numbers of propellers are required for the body to accomplish its mission.

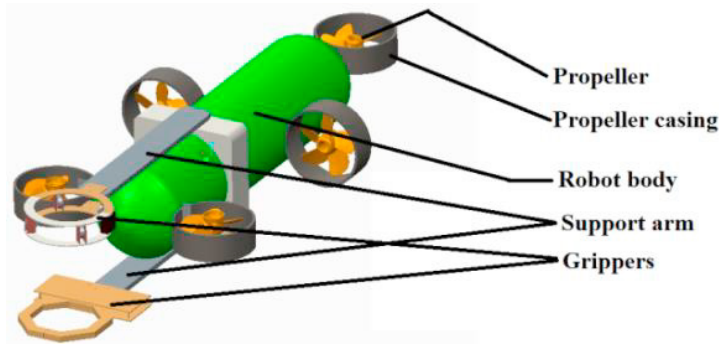


Fig. 2. The underwater robot CAD model.

Table 1. Geometry of proposed Underwater Robot

Part	Parameter	Dimensions
Body (Material: PVC)	body length (m)	0.30
	body diameter (m)	0.075
	Motor diameter (m)	0.04
	Shaft diameter (m)	0.006
Thruster (DC geared Motor)	Motor length (m)	0.04
	Gear ratio	1 : 3
	Propeller diameter (m)	0.09
Thruster (GM Magnesium alloy sheet Propeller)	Number of blades	4
	Thickness (m)	0.0003
	Blade length (m)	0.035
	Blade angle (0)	230
Gripper (Material: Acrylic polymer)	Casing diameter (m)	0.01
	Thickness(m)	0.003
	Inner diameter(m)	0.17
Pipe line setup (Material: PVC)	Outer diameter(m)	0.23
	Pipe diameter(m)	0.15
	Pipe thickness(m)	0.005
	Pipe length(m)	0.9144

The grippers are designed to holding/release and clinging along the pipe during inspection process. Acrylic polymer sheet is used as material for grippers in this study. This is due to its light weight so that less energy can be consumed. It is noted that additional buoyancy is created in the presence of grippers and hence final prototype design is carefully considered for stability.

2.2. Test motion

The underwater robot is tested for surge and heave motion. The speed is analyzed after sufficient balancing requirements to maintain the body at a certain depth. The motion is carried out using DC motors connected to propellers for appropriate directions. A two-way switch is used initially for manual testing, which later is converted to programmed testing. Figure 3 shows the schematic of movements involved in a underwater robot with grippers.

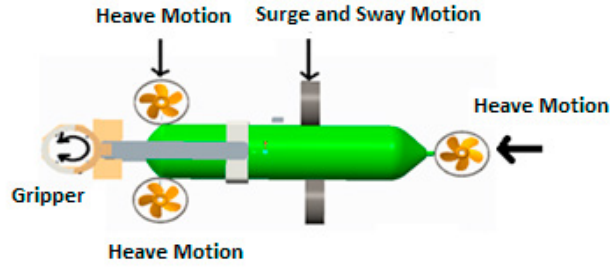


Fig. 3. The underwater robot motion testing.

2.3. Computational Fluid Dynamics

The simplified underwater robot model is used for CFD simulation. The underwater model has two arms connected to grippers as shown in the Figure 4. Half a million elements in the mesh is selected after testing [10,12].

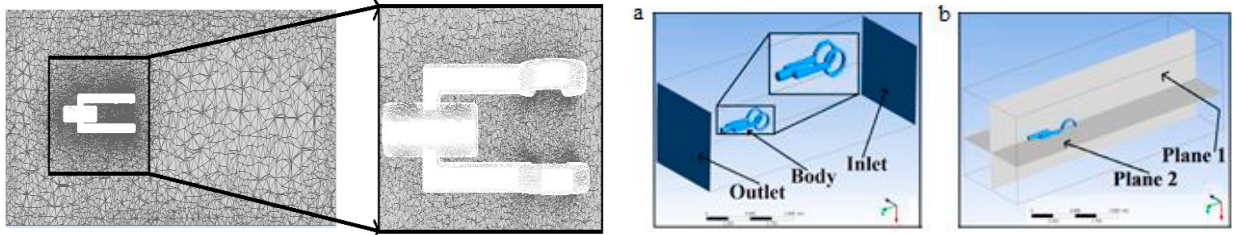


Fig. 4. Mesh model of underwater robot with grippers (inset) in meshing and (a) Underwater robot body in boundary conditions (b) test reference planes of underwater robot.

Underwater robot with boundary conditions and test reference planes are shown in the fig 4 (a) and (b). To simulate the underwater robot, a UDF is written for a turbulent flow (to capture unsteadiness in flow) and fed to the CFD solver. The mathematical equations incorporated in the simulation process are explained below.

For the flow considered in this study, the conservation equations for mass and momentum are solved.

The equation for conservation of mass, or continuity equation, can be written as follows:

$$\frac{\partial \rho}{\partial t} + \nabla \cdot \rho \vec{v} = 0 \tag{1}$$

The conservation of momentum in an inertial (non-accelerating) reference frame is described by

$$\frac{\partial}{\partial t} (\rho \vec{v}) + \nabla \cdot (\rho \vec{v} \vec{v}) = -\nabla p + \nabla \cdot (\bar{\tau}) + \rho \vec{g} \tag{2}$$

Where p is the static pressure, $\bar{\tau}$ is the stress tensor (described below), and $\rho \vec{g}$ is the gravitational body force. The stress tensor $\bar{\tau}$ is given by

$$\bar{\tau} = \mu \left[(\nabla \vec{v} + \nabla \vec{v}^T) - \frac{2}{3} \nabla \cdot \vec{v} I \right] \tag{3}$$

Where μ is the molecular viscosity, I is the unit tensor, and the second term on the right hand side is the effect of volume dilation.

Turbulence Modeling

The exact transport equations for the transport of the Reynolds stresses, $\overline{\rho u_i' u_j'}$, is written as follows:

$$\begin{aligned} \frac{\partial}{\partial t} (\overline{\rho u_i' u_j'}) + \frac{\partial}{\partial x_i} (\overline{\rho u_k u_i' u_j'}) = & - \frac{\partial}{\partial x_k} \left(\frac{\mu_t}{\sigma_k} \frac{\partial \overline{u_i' u_j'}}{\partial x_k} \right) + \frac{\partial}{\partial x_k} \left(\mu \frac{\partial}{\partial x_k} (\overline{u_i' u_j'}) \right) - \rho \left(\overline{u_i' u_k} \frac{\partial u_j}{\partial x_k} + \overline{u_j' u_k} \frac{\partial u_i}{\partial x_k} \right) - \\ & \frac{\mu_t}{\rho Pr_t} \left(g_i \frac{\partial T}{\partial x_j} + g_j \frac{\partial T}{\partial x_i} \right) + p \left(\frac{\partial u_i'}{\partial x_j} + \frac{\partial u_j'}{\partial x_i} \right) - 2\mu \left(\frac{\partial u_i'}{\partial x_k} \frac{\partial u_j'}{\partial x_k} \right) + 2\rho \Omega_k (\overline{u_j' u_m'} \epsilon_{ikm} + \overline{u_i' u_m'} \epsilon_{jkm}) \end{aligned} \tag{4}$$

In general, when the turbulence kinetic energy is needed for modelling a specific term, it is obtained by taking the trace of the Reynolds stress tensor:

$$k = \frac{1}{2} \overline{u_i' u_i'} \tag{5}$$

A transport equation is solved for the turbulence kinetic energy in order to obtain boundary conditions for the Reynolds stresses. In this case, the following model equation is used:

$$\frac{\partial}{\partial t}(\rho k) + \frac{\partial}{\partial x_i}(\rho k u_i) = \frac{\partial}{\partial x_j} \left[\left(\mu + \frac{\mu_t}{\sigma_k} \right) \frac{\partial k}{\partial x_j} \right] + \frac{1}{2} [P_{ii} + G_{ii}] - \rho \epsilon (1 + 2M_t^2) \tag{6}$$

Where $\sigma_k = 0.82$, turbulent Mach number, $M_t = k/0.5/a$, a being the speed of sound.

The scalar dissipation rate, ϵ , is computed with a model transport equation

$$\frac{\partial}{\partial t}(\rho \epsilon) + \frac{\partial}{\partial x_i}(\rho \epsilon u_i) = \frac{\partial}{\partial x_j} \left[\left(\mu + \frac{\mu_t}{\sigma_\epsilon} \right) \frac{\partial \epsilon}{\partial x_j} \right] C_{\epsilon 1} \frac{1}{2} [P_{ii} + C_{\epsilon 3} G_{ii}] \frac{\epsilon}{k} - C_{\epsilon 2} \rho \frac{\epsilon^2}{k} \tag{7}$$

Where $\sigma_\epsilon = 1.0, C_{\epsilon 1} = 1.44, C_{\epsilon 2} = 1.92, C_{\epsilon 3}$ is evaluated as a function of the local flow direction relative to the gravitational vector

The turbulent viscosity, μ_t , is computed as

$$\mu_t = \rho C_\mu \frac{k^2}{\epsilon} \tag{8}$$

Where $C_\mu = 0.09$.

The turbulence model requires boundary conditions for individual Reynolds stresses, $\overline{u_i' u_i'}$ and for the turbulence dissipation rate, ϵ . These quantities can be input directly or derived from the turbulence intensity and characteristic length. The CFD study gives information about the hydrodynamic pressure and drag. This is required for arriving at a final prototype in the experimental study. For testing the prototype with different motion, the hardware development and control system is crucial and described in the next section.

3. Software and Hardware Architecture

The software architecture is divided into two parts; python programming for Raspberry Pi operation and control, and embedded C programming for Arduino operation and control. Arduino is used to control the hardware (propellers and sensors) of the underwater robot. The robot motion control, sensors and grippers controllers are connected to Arduino. Raspberry Pi takes care of the vision system for image capturing [13,14] and establishing communication between underwater robot and personal computer. The Raspberry Pi and Arduino are interfaced suitably to establish a stable connection between these controllers. The control system implemented in the underwater robot is of distributed type. This control system provides flexible and fast control over the operation (motion and inspection) of the underwater robot. The Raspberry Pi and Arduino controllers are connected to personal computer through Universal Serial Bus (USB) for communication as shown in Figure 5.

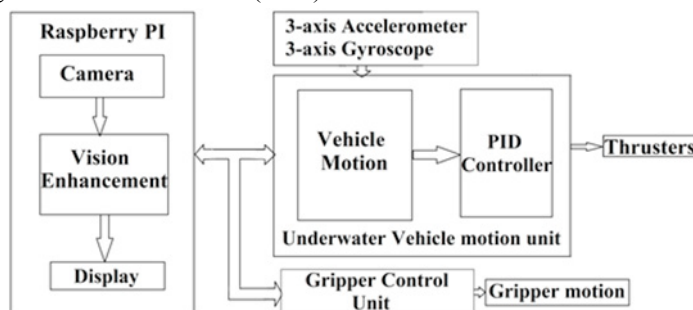


Fig. 5. Overall control system architecture.

4. Results and Discussion

4.1. Experimental study

Based on the study so far carried out, several parameters that are necessary to develop the underwater robot like buoyancy, weight distribution, shape of body, orientation, propeller etc are identified. Many preliminary studies have been carried out to develop the most suitable underwater vehicle that can help in the inspection process. One of the

major factors to stabilize the body is weight distribution. Figure 6(a) and Figure 6(b) shows the process of weight balancing and distribution during preliminary tests. The final prototype is shown in Figure 7(a) and its testing in water tank in Figure 7(b). The drag force F_D is calculated using formula as in Eqn. 9. From the experimental studies, the forward motion velocity is 0.1m/s and the drag force F_D is found to be 0.006 N shown in Table 2. The images output from HD camera at different times during inspection are shown in Figure 8 (a) and (b).

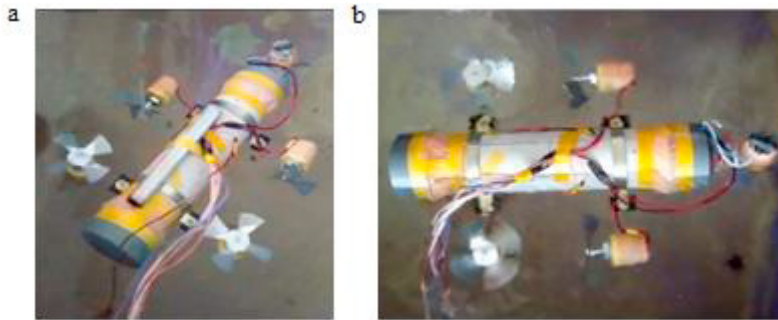


Fig. 6. (a) preliminary study (weight placed outside); (b) preliminary study (weight placed inside).

$$\text{Drag Force } F_D = \frac{1}{2} \rho v^2 C_d A \tag{9}$$

Where ρ is density of fluid (water-998kg/m³); v is velocity of body (0.1m/s); C_d is the drag coefficient [15] of the surface (0.295) and A is the area of the surface contact with fluid flow (0.0089m²).

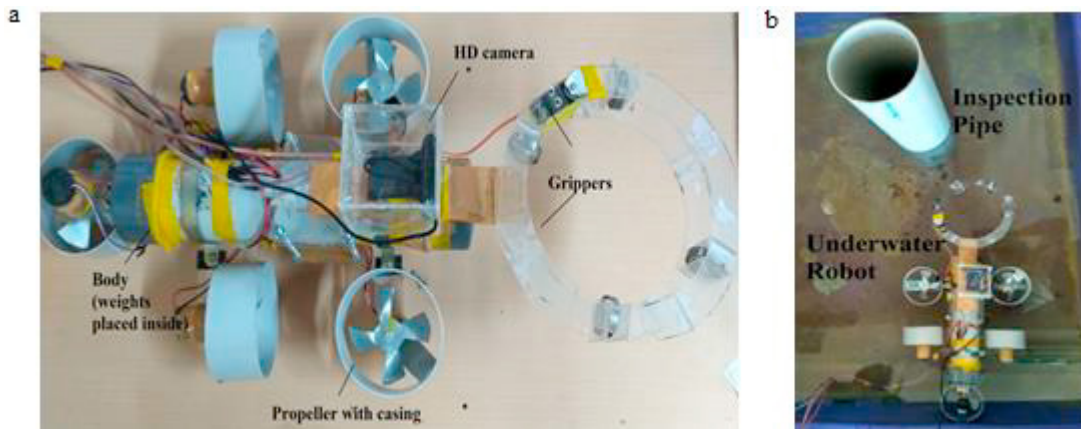


Fig. 7 (a) Final prototype of the underwater robot; (b) the testing of underwater robot in water tank.

Table 2. The underwater robot experimental results (without gripper)

Motion	Speed
Heave	0.2m/s
Sink	0.1m/s
Surge	0.1m/s
Yawing (turning for 90o angle)	0.105 rad/s
Drag force	0.006N

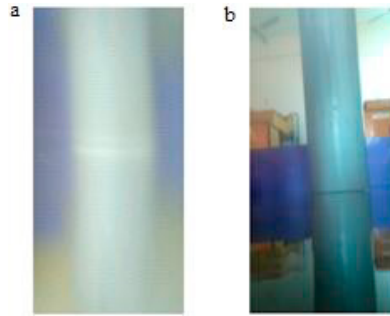


Fig. 8 (a) Output from the robot HD camera when it was fully submerged; (b) Output from the robot HD camera from the surface.

4.2. CFD Study

The computational fluid dynamic study is carried out with simplified underwater robot model after checking the sufficient mesh requirements. For the unsteady motion, the time step is also varied to suit the dynamic mesh conditions. The pressure and velocity contours at reference planes are shown in Figure 9 (a) and 9(b). Wake region is captured [16] during the horizontal travel at specified depth as shown in Figure 9(c) and 9(d). From CFD, the profile drag of the body motion at 0.1 m/s (derived from experiments) for the specified time period is found as 0.0057 N. The drag force from experimental results is from underwater vehicle without gripper but the drag force from simulation is belongs to underwater vehicle with gripper. The simulated value and experimental value are very close in range, shows the speed drop of underwater vehicle with gripper is negligibly less.

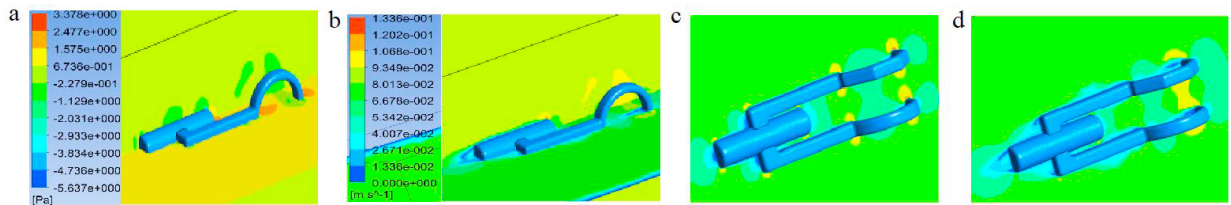


Fig. 9. (a) Pressure contour in test plane; (b) velocity contours in test plane; (c) Velocity contour at time = 0.4s; (d) velocity contour at time = 4.2s.

4.3. Cost Analysis

The cost estimation is carried out based on the items used for the project [17] that are available locally. The total cost estimated to develop the underwater robot is shown in the Table 3 below.

Table 3. Cost estimation

Item	Cost (in Indian Currency, INR)
Raspberry Pi 3	4000
Arduino Uno	450
Gyroscope and Accelerometer (MPU6050)	300
12v Switched Mode Power Supply	150
Prototype Fabrication	1500
HD Camera	1000
12v DC motors (5 nos.), Servo Motor (2 nos.)	1050
Miscellaneous (Wires, glue gun, soldering etc.)	1600
Total	10000

5. Conclusion

The conceptual CAD model of the underwater robot is designed after the outcome on literature studies. Several preliminary studies are carried out to test buoyancy and stability on the underwater body. The final designed prototype is arrived after CFD simulations compared as to its previous version. The drag force and velocity are calculated and found to be similar between CFD and experimental studies. The CFD analysis is carried out with an UDF for the motion of a simplified underwater robot. The drag force calculated from the CFD analysis and experiments are within 5 % satisfactory level of agreement. Further, the image was captured using the underwater robot camera and hence the proposed mission is accomplished. However, further work on gripping force requirements and its corresponding energy consumption study is needed. The stress induced by gripper on the pipe can be analyzed for different gripper materials in the future work.

References

- [1] The ROV Manual: A user guide for Remotely Operated Vehicles, second edition, 2014.
- [2] Zain, ZainahMd, Maziyah Mat Noh, KhairulAshraffAb Rahim, and NurfadzillahHarun (2016). "Design and Development of an X4-ROV." *IEEE International Conference on Underwater System Technology: Theory and Applications (USYS)*:207–211.
- [3] Spadafora, Muzzupappa, Bruno, Ribas, and Ridao (2015). "Design and Construction of a Robot Hand Prototype for Underwater Applications." *IFAC-PapersOnLine* 48(2): 294–299.
- [4] Hasan, Nazmul, MdSyadusSefat, and MdShahjahan (2017). "A low cost remotely operated vehicle for underwater surveillance—A complete experimental platform." *International Conference on Electrical, Computer and Communication Engineering (ECCE)*: 486–490.
- [5] Anwar, Inzamam, OwaisMohsin, SaqibIqbal, ZainUlAbideen, Attique Ur Rehman, and Nisar Ahmed (2016). "Design and fabrication of an underwater remotely operated vehicle (Single thruster configuration)." *13th International Bhurban Conference on Applied Sciences and Technology (IBCAST)*:547-553.
- [6] Mai, Christian, Simon Pedersen, Leif Hansen, Kasper L. Jepsen, and Zhenyu Yang (2016). "Subsea infrastructure inspection: A review study." *IEEE International Conference on Underwater System Technology: Theory and Applications (USYS)*:71–76.
- [7] <http://www.offshore-mag.com/articles/print/volume-76/issue-3/flowlines-and-pipelines/computed-tomography-offers-effective-tool-for-subsea-pipeline-inspection.html>
- [8] Pranesh, Sathianarayanan, Chandrasekar, Murugesan, Ramadass, and Atmanand (2015). "Design and development of polypropylene frame for remotely operated vehicle." *OCEANS 2015-Genova* :1–6.
- [9] Joochim, Chanin, RattanakornPhadungthin, and SawangtitSrikitsuwan (2015). "Design and development of a Remotely Operated Underwater Vehicle." *16th International Conference on Research and Education in Mechatronics (REM)*: 148–153.
- [10] Leong, Ranmuthugala, Forrest, and Duffy (2015). "Numerical investigation of the hydrodynamic interaction between two underwater bodies in relative motion." *Applied Ocean Research* 51:14–24.
- [11] Kumaravelu, Giridharan, ChetanSoni, and Shunmugham R. Pandian (2016). "Design of a compact and economical remotely operated vehicle for aquatic monitoring." In *Region 10 Conference (TENCON)*:1834–1838.
- [12] Leong, ZhiQuan, DevRanmuthugala, Irene Penesis, and Hung Duc Nguyen (2012). "Computational fluid dynamics re-mesh method to generating hydrodynamic models for maneuvering simulation of two submerged bodies in relative motion." *Journal of Computer Science and Cybernetics* 27(4) 353–362.
- [13] Choi, Jinwoo, Yeongjun Lee, Taejin Kim, Jongdae Jung, and Hyun-Taek Choi (2017). "Development of a ROV for visual inspection of harbor structures." *IEEE conference on Underwater Technology (UT)*: 1–4.
- [14] Narimani, Mehdi, SorooshNazem, and Mehdi Loueipour (2009). "Robotics vision-based system for an underwater pipeline and cable tracker." *IEEE conference on Oceans 2009-Europe*: 1–6.
- [15] Fluid Mechanics, Frank M. White, McGraw-Hill Education 8th edition, 2015.
- [16] Leong, ZhiQuan, Dev Ranmuthugala, Irene Penesis, and Hung Nguyen(2015). "Quasi-static analysis of the hydrodynamic interaction effects on an autonomous underwater vehicle operating in proximity to a moving submarine." *Ocean Engineering* 106: 175–188.
- [17] Satish Kumar, ArockiaSelvakumar, and PratibhaNalini (2016). "Development of Autonomous Robot for Underwater Applications", *International Journal of Control Theory and Applications* 9 (13): 6249-6260.